Combining Low-Emissivity Thin Coating and 3D-Printed Original Designs for Superior Fire-Protective Performance

Laura Geoffroy, Anne-Lise Davesne, Fabrice Parent, Frédéric Sanchette, Fabienne Samyn, Maude Jimenez, Serge Bourbigot

ACS OMEGA

Article

Combining Low-Emissivity Thin Coating and 3D-Printed Original Designs for Superior Fire-Protective Performance

Laura Geoffroy, Anne-Lise Davesne, Fabrice Parent, Frédéric Sanchette, Fabienne Samyn, Maude Jimenez, and Serge Bourbigot*

Cite This: https://dx.doi.org/10.1021/acsomega.0c02902

Read Online

ACCESS | Metrics & More | Article Recommendations

ABSTRACT: Three-dimensional (3D) printing is a very flexible process to design various objects of original shapes. Previous works highlighted the preparation of new multimaterials composed of an original sandwich structure made of the ethylene vinyl acetate copolymer containing 30 wt % of aluminum trihydroxide in which a hydrogel phase made of agar and vermiculite was incorporated. This original material revealed an extremely low heat release rate (HRR) (with a reduction of 86 and 64% with regard to the peak of the HRR and total heat release, respectively, when compared to the same sample without hydrogel filling) during its heat exposure at 50 kW/m^2 according to the mass loss cone calorimetry test.
However, the time to ignition (TTI) of this material was not improved. This work consequently focuses on delaying the time to ignition of this hydrogel sandwich 3D-printed multimaterial. Solution consists in depositing by pulsed DC magnetron sputtering a low-emissivity thin coating on the exposed skin surface. This coating reflects most of the infrared rays responsible for heat absorption and thus delays the ignition of the underlying material. The thermal resistance performances of this coated sandwich 3D-printed multimaterial were evaluated, and a mechanism of action was proposed to explain the dramatic enhancement of the properties.
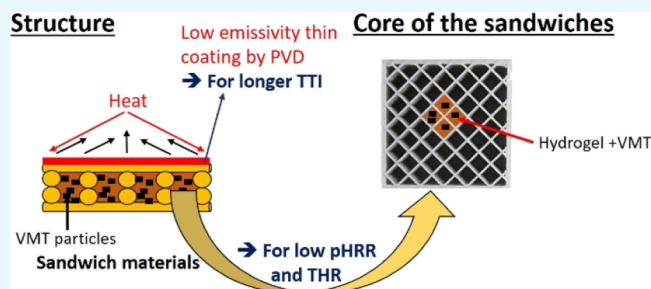
1. INTRODUCTION

Polymeric materials are widely used as they present many advantages. In particular, they have low mass, allowing to synthesize lightweight structures. Polymers are also easily prepared using various processes such as extrusion, injection, and additive manufacturing. However, the main drawback of these materials is their high flammability, which creates safety issues. For this reason, many works focused on the improvement of their fire behavior. Different approaches can be considered. Some of them investigate, for example, the modification of the materials chemistry by adding flame-retardant additives to improve their fire-protective properties.[1−4] The approach selected in this work is a new way of thinking. Instead of changing the materials formulation, the design or the assembly of materials is investigated to achieve a better fire behavior. The three-dimensional (3D) printing process fits well for such developments and to conceive original design, as it was previously demonstrated in ref 5. This approach is particularly interesting in the context where chemical fire retardants are under scrutiny because of increasing environmental and health concerns.

In previous work carried out in our lab, it was proven that a flame-retarded formulation composed of the ethylene-vinyl acetate (EVA) copolymer with 30 wt % of aluminum trihydroxide (ATH) can be 3D printed.[6] Following this

research, an innovative sandwich design was achieved. It is composed of two skins completely filled with a polymer (EVA/ATH (30 wt %)) and a core partially filled with 30% of the polymer (Figure 1). To reach even better fire protection, the empty cells of this structure were filled in with different phases such as liquid, solid, and hydrogel[5,7] to synthesize new sandwich multimaterials. Based on our previous paper,[7] a hydrogel phase composed of agar and vermiculite (VMT) revealed the best thermal resistance performances while being easily processed. Under high-temperature stress (radiative heat flux) conditions, VMT particles organized in a network exhibit high tortuosity, slowing down the gas emission from polymer decomposition. Therefore, the flame is quickly extinguished and the heat release rate (HRR) is dramatically reduced. Nevertheless, the time to ignition (TTI) of material is short, even if the extinguishment occurs rapidly after ignition. The aim of this study is, therefore, to improve the TTI of these samples, via a surface treatment, in order to combine low peak
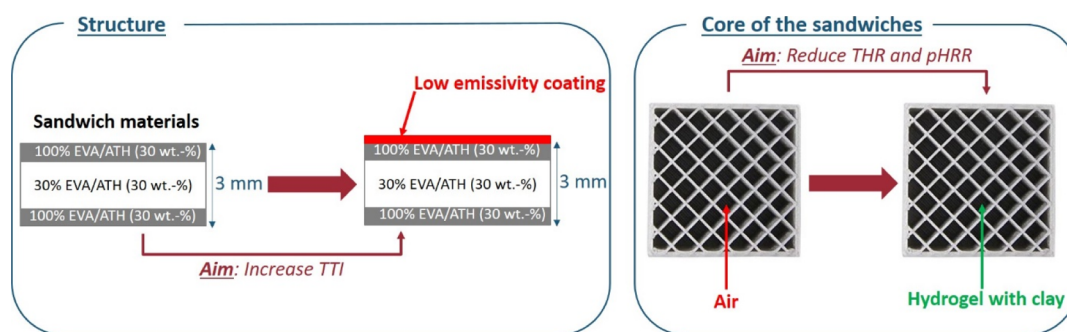
Figure 1. Concept of low-emissivity hydrogel sandwich flame-retardant design printed using additive manufacturing.

of HRR (pHRR) and total heat release (THR) with a low ignitability. One of the methods reported to delay TTI is to reflect infrared (IR) rays responsible for radiative heat transfer by using highly reflective heat coatings, that is to say coatings with a low emissivity. While this approach may not work that well in convective and conductive fire scenarios,[8] it is very efficient against a radiant heat flux like this study is concerned with. The first study on that system was undertaken by Schartel et al. in 2011 on polycarbonate and polyamine 6.6. A trilayer composed of chrome, copper, and silicon dioxide (Cr/Cu/SiO$_2$) reduced the flammability indexes on both substrates.[9] Then, in 2014, Försth et al. took over this method using indium tin oxide (ITO) on poly(methyl methacrylate) (PMMA) and vanadium dioxide (VO$_2$) on steel. However, these systems did not reach the low emissivity obtained with copper.[10] Recently, Davesne et al. studied the combination of a thin layer of metal such as aluminum, protected by a dielectric such as alumina on polypropylene and polyamine 6, which revealed an interesting behavior upon heating.[11]

In this paper, the influence of such low-emissivity coating (composed of aluminum protected by alumina) on sandwich 3D-printed materials was first determined. Then, this coating was deposited on hydrogel sandwich 3D-printed multimaterials to examine its potential influence on TTI of the material. Full characterization of samples (emissivity, mass, and hydrogel amount) was carried out, and all samples were then tested by mass loss cone calorimetry (MLCC) under a 50 kW/m^2 external heat flux. Finally, the fire protection mechanism was investigated.

2. RESULTS AND DISCUSSION

2.1. Characterization before Fire Testing. All samples studied (fully described and named in the Materials and Methods part) were characterized before fire testing (Table 1 and Figure 2). As illustrated in Figure 2, the top section of samples 3D-air and 3D-hydrogel (H) B + VMT looks the same. The only difference is the presence of H B + VMT in the

cells present in the sandwich core. Considering the coated samples (i.e., IR-3D-air (Figure 2b) and IR-3D-H B + VMT (Figure 2d)), homogeneous deposits presenting mirror aspects are observed on both surfaces.

According to Table 1, the thickness and mass of the materials with air, that is, 3D-air and IR-3D-air, are roughly equal to 3 mm and 7.2 g, respectively. For the hydrogel sandwich multimaterials, that is, 3D-H B + VMT and IR-3D-H B + VMT, the thickness, mass, and hydrogel mass of the design are the same and equal to 3 mm, 11.3, and 4.1 g, respectively. Meanwhile, the top section emissivity of the coated samples was measured (Table 1) and compared. It is noteworthy to point out the significant emissivity decrease between the samples without surface treatment and the samples with a metallic coating. Hence, the reflection of IR rays is enhanced, and it can be expected that the heat absorption during exposure to a radiative thermal constraint should be decreased.

Finally, the composition of the low-emissivity coating and its thickness were analyzed using scanning electron microscopy-energy dispersive X-ray spectroscopy (SEM-EDS) (Figure 3). Al, O, and Si-mappings were done on the cross-section of low-emissivity coating deposited on a glass slide, as illustrated in Figure 3. The O element distribution was analyzed to distinguish the Al$_2$O$_3$ layer from Al, which is composed of the low-emissivity coating (Figure 3a). Al element repartition was observed to identify the coating and its thickness (Figure 3b). The Si element was also analyzed to locate the glass slide on which the low-emissivity coating is deposited (Figure 3c). These analyses first revealed that the low-emissivity coating is well composed of aluminum and alumina layers. Indeed, during the physical vapor deposition (PVD) process, a homogeneous layer of Al was first deposited on a glass slide with a thickness of 0.490 μm on which a homogeneous layer of Al$_2$O$_3$ having a thickness of 0.093 μm is coated. No delamination or bubbles are observed between both layers.

2.2. Fire Testing. Figure 4 illustrates the comparison of the HRR as a function of time (Figure 4a) and the temperature increase versus time (Figure 4b) for each material. Table 2 shows the three main parameters determined from the HRR versus time curve illustrated in Figure 4a.

First of all, it is observed that the incorporation of H B + VMT dramatically reduces the THR and the pHRR of materials. Indeed, for 3D-H B + VMT, the THR and pHRR are reduced by 85 and 51%, respectively, compared to 3D-air. As regards the TTI, a slight improvement by 8 s (about 1.36 times longer) is observed when compared to the sample with air (3D-air). The addition of a low-emissivity coating allows considerably delaying the TTI. Indeed, the TTI jumps from 22 s for 3D-air to almost 6 min for IR-3D-air. However, in terms

Table 1. Quantitative Values of Each Sandwich Multimaterial Studied

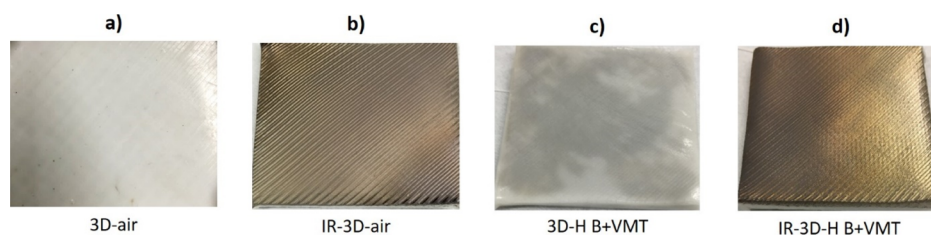| polymer matrix	mass (g)	thickness (mm)	hydrogel amount (g)	emissivity
3D-air	6.5 ± 0.9	3 ± 0		0.96 ± 0.00
IR-3D-air	7.89 ± 0.08	3.1 ± 0.2		0.21 ± 0.03
3D-H B + VMT	11.2 ± 0.8	3 ± 0.2	4.1 ± 0.3	0.96 ± 0.00
IR-3D-H B + VMT	11.5 ± 0.1	3.1 ± 0.1	4.17 ± 0.08	0.19 ± 0.04

Figure 2. Top section pictures of each sandwich multimaterial studied (a) 3D-air, (b) IR-3D-air, (c) 3D-H B + VMT, and (d) IR-3D-H B + VMT).
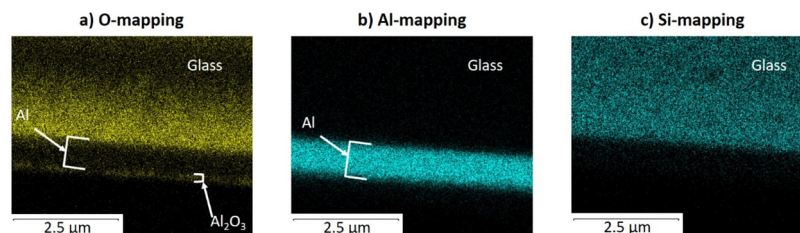

Figure 3. Cross-sectional X-ray mapping of (a) O element, (b) Al element, and (c) Si element of the low-emissivity coating deposited on a glass slide investigated using SEM−EDS analysis.
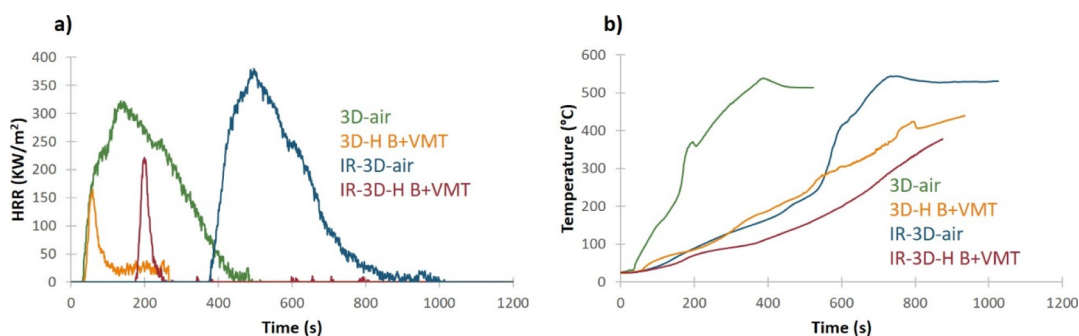

Figure 4. Fire behavior of each material studied (a) HRR vs time and (b) temperature increase vs time.

Table 2. Fire Protection Performance Values of Each Material Studied

Polymer matrix	TTI (s)	THR (MJ/m^2)	pHRR (kW/m^2)
3D-air	22 ± 3	55 ± 3	249 ± 10
IR-3D-air	340 ± 35 (x15.5)	61 ± 4 (11%)	283 ± 2 (14%)
3D-H B+VMT	30 ± 6 (x1.36)	8 ± 2 (-85%)	122 ± 12 (-51%)
IR-3D-H B+VMT	184 ± 11 (x8.36)	4.7 ± 0.2 (-91%)	152 ± 13 (-64%)

of THR (11%) and pHRR (14%), no improvement is observed compared to 3D-air.

By combining the low-emissivity coating and hydrogel in the core voids, the fire behavior is dramatically enhanced. The THR and pHRR differences between IR-3D-H B + VMT and 3D-air are −91 and −64%, respectively, with a high increase of TTI by 162 s (about 8.36 times longer, which corresponds to a jump from 22 s up to 3 min). This increase of TTI is not as huge as observed for the coated sandwich without hydrogel (IR-3D-air). For both samples, ignition occurs when combustible gases are released. The low-emissivity coating acts as a reflective barrier against IR by slowing down the heat propagation in the sample. However, when the EVA/ATH decomposition temperature is reached, gases are released, which create a pressure, damaging the low-emissivity coating and leading to cracks. As a consequence, the coating loses its protective property, and ignition occurs. In the presence of

hydrogel (IR-3D-H B + VMT), water vapor is released in addition to decomposition gases from EVA/ATH. Therefore, higher pressure is reached and an earlier failure of coating is observed, which explains the lower TTI measured for this system compared to IR-3D-air. However, thanks to the H B + VMT and especially to the VMT orientation, the flame quickly extinguishes, which explains the low THR and pHRR recorded during the MLCC test.

During the MLCC tests, the temperature increase was measured using a thermocouple at the backside of the material (Figure 4b). When the reference 3D-air is exposed to heat, the backside temperature increases quickly, with a slope equal to 1.7 °C/s, and reaches a steady-state temperature of 500 °C. For IR-3D-air, the increase in temperature is slowed down more than 4 times, with a slope of 0.4 °C/s. Before the sample ignition, the temperature is never higher than 200 °C. This slow temperature increase is explained by the low-emissivity
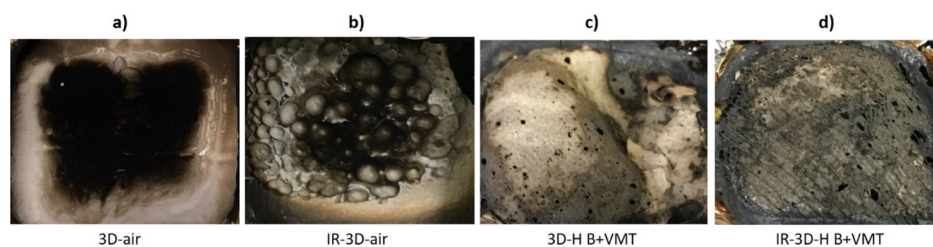
Figure 5. Top surface residue pictures of each material studied (a) 3D-air, (b) IR-3D-air, (c) 3D-H B + VMT, and (d) IR-3D-H B + VMT).
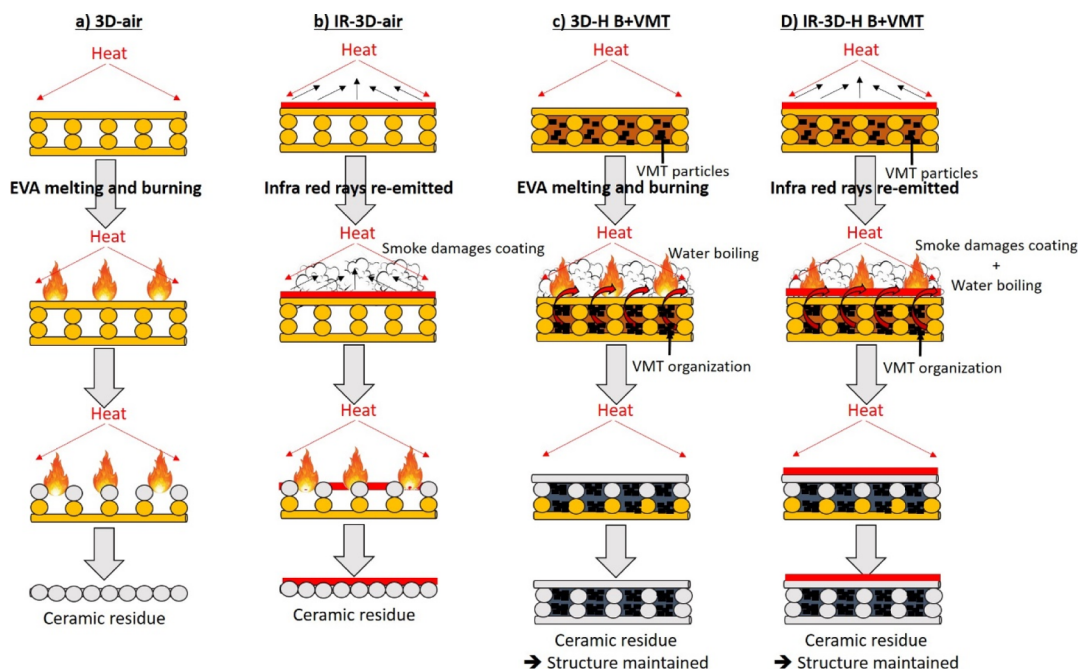

Figure 6. Illustration of the fire behavior mechanism of each sandwich multimaterial studied (a) 3D-air, (b) IR-3D-air, (c) 3D-H B + VMT, and (d) IR-3D-H B + VMT).

coating, which limits the heat absorption, leading to a delayed ignition. After 500 s, ignition occurs and the temperature increases rapidly, with a slope of 2.4 °C/s, and reaches 500 °C after 700 s of heat exposure. Regarding 3D-H B + VMT, a slow temperature increase, with a slope equal to 0.5 °C/s (3.4 times lower than the slope obtained for 3D-air), is observed during the whole MLCC test. It can be explained by the presence of H B + VMT. According to ref 7, VMT particles present in the hydrogel phase have a preferential orientation. When the sample with H B + VMT is exposed to heat, the water contained in hydrogel boils. The VMT particles form quickly a gradient of tight stack of VMT. This tight layer of VMT acts as an efficient physical barrier, which slows down the gas emission from polymer decomposition that feeds the flame. As a consequence, the flame is fast extinguished and low THR and pHRR are measured, which justifies the slow temperature increase, compared to the reference 3D-air. Finally, by the combination of low-emissivity coating and H B + VMT, an even slower increase in temperature is observed during the MLCC test. Indeed, from 200 to 400 s, a plateau at 100 °C is observed for IR-3D-H B + VMT. After 400 s, temperature goes up, with a low slope equal to 0.6 °C/s. Therefore, the low-emissivity sandwich multimaterial designed in this work allows obtaining (i) a very low heat release (fast flame extinguishment), (ii) a longer TTI, and (iii) a high thermal gradient

between the top and backside of the sample, with a very slow temperature increase.

After heat exposure, the top section of the residues of each material was observed (Figure 5). On the one hand, only agglomerated powder remains after the fire test for 3D-air and IR-3D-air. Both residues contain alumina from ATH dehydration and for the coated sample, additional alumina with aluminum (mainly oxidized[11]) from the low-emissivity coating. On the other hand, Figure 5 shows that the design initially created is retained for the samples containing hydrogel B, both coated and uncoated: the top section is visibly kept for both samples. This point can be explained by the presence of VMT in hydrogel, which agglomerates on the polymer walls and thus maintains the initial structure (formation of an exoskeleton), as it was demonstrated in a previous paper.[11] The only difference between these samples is the color of the top section. A gray color is observed for IR-3D-H B + VMT, compared to a yellowish color for 3D-H B + VMT. This observation makes sense and results from the presence of the low-emissivity coating, which remains in place during the test and is mostly composed of aluminum and aluminum oxides at this point.[11]

2.3. Mechanism of Action. The fire behavior of each material is illustrated in Figure 6. For the reference 3D-air, when the material is exposed to a radiative thermal constraint, the sample ignites, starts to melt, and decomposes: all voids

then collapse (Figure 6a). Therefore, the design is not retained and no improvement in terms of TTI, THR, or pHRR is measured. When a low-emissivity coating is deposited on the top surface on the sample (IR-3D-air), it reflects the IR rays, which significantly delay the TTI (Figure 6b). However, when the backside of the sample reaches 200 °C, the polymer starts to melt and decompose, releasing gases. On the one hand, the polymer melting damages the design initially achieved. On the other hand, the gases released by the polymer decomposition weaken the coating (creation of an internal pressure at the interface coating—decomposing polymer), which leads to the ignition and the decomposition of the whole sample. Therefore, the only effect of the low-emissivity coating is to lengthen the TTI, but when the sample ignites, no reduction of THR of pHRR is recorded. For 3D-H B + VMT, as it was previously explained in ref 7 when the sandwich multimaterial is exposed to heat, ignition occurs rapidly, but because of the water and VMT particles contained in hydrogel, the flame extinguishes rapidly (Figure 6c). Indeed, the water in the hydrogel phase is released slowly. At the same time, VMT particles organize upon heating and form a protective barrier constituted by the accumulation of VMT platelets that prevents the gases coming from polymer decomposition to feed the flame. Therefore, very low THR and pHRR are measured during the MLCC test, and the design initially achieved is maintained. However, the TTI of this sandwich multimaterial is not improved. Finally, when IR-3D-H B + VMT is exposed to heat, the low-emissivity coating reflects most of the IR rays (Figure 6d). Simultaneously, the water contained in the hydrogel phase starts to boil when 100 °C is reached, which causes the top section of the material to swell, and this swelling creates cracks in the coating, ultimately leading to ignition. However, as for 3D-H B + VMT, the flame extinguishes rapidly with the combined action of water and VMT particles contained in the hydrogel. Therefore, by combining both concepts, that is, low-emissivity coating and sandwich multimaterials design, fire-protective performances are dramatically enhanced, characterized by a very low THR and pHRR and a longer TTI.

3. CONCLUSIONS

Two concepts were combined in this work: i) the reduction of the surface emissivity through the use of a thin metal/dielectric coating, which significantly improves the TTI of materials by reflecting IR rays to limit radiative heat transfer, and ii) the sandwich multimaterial design, which decreases the HRR by combining various phases using an original 3D-printed design. This novel work allows reaching superior fire retardancy through the new design achieved instead of only modifying the material formulation and chemistry.

4. MATERIALS AND METHODS

4.1. Preparation of 3D-Printed Sandwich Multi-materials. *4.1.1. Materials.* EVA (Evatane 28-05, Arkema, Colombes, France) is used as a polymer matrix. 30 wt % ATH (Apyral 40CD, Nabaltec, Schwandorf, Germany) was added to EVA to obtain the EVA/ATH (30 wt %) material. This material was extruded at 100 rpm using a corotative twin-screw extruder (Thermo Scientific Rheomex OS PTW16 Haake, Vreden, Germany) with the following temperature profile in the ten zones from the feeder to die: 150, 160, 160, 160, 170, 170, 170, 160, 160, and 150 °C. The ATH additive was

incorporated into zone 4 and the polymer string coming out was air cooled at room temperature and finally pelletized (pelletizer Thermo Scientific, Waltham, Massachusetts, United States of America).

4.1.2. Preparation of 3D-Printed Materials. The previously prepared pellets were used to feed the 3D printer (Pollen, Ivry-sur-Seine, France), fully described elsewhere.[6] They go through a monoscrew extruder where a thermal gradient from 65 to 225 °C occurs. Because of the thermal gradient and shear strain, the polymer is fused and deposited on a heating plate at 65 °C. The heating plate moves at 20 mm/s, which allows building the 3D object layer by layer. A sandwich design is conceived and composed of two skins completely filled with the EVA/ATH (30 wt %) polymer, and a core partially filled with 30% of the EVA/ATH (30 wt%) material and thus 70% of holes, as illustrated in Figure 1. According to the samples studied (Table 3), (i) the empty cells created by the design are

Table 3. Description and Composition of Materials Studied

name of the samples	top section		core composition
	material	low-emissivity coating	
1 3D-air		no	air
2 IR-3D-air		yes	air
3 3D-H B + VMT	EVA/ATH (30 wt %)	no	hydrogel: agar + VMT
4 IR-3D-H B + VMT		yes	hydrogel: agar + VMT

filled with hydrogel composed of agar and VMT and named H B + VMT (H B + VMT preparation fully described in Section 4.1.4), as it is the case for IR-3D-H B + VMT and for 3D-H B + VMT (Figure 7), and (ii) a low-emissivity coating is deposited on the top skin of the design using a PVD process, more specifically by pulsed DC magnetron sputtering (fully described in Section 4.1.3), as it is the case for IR-3D-air and for IR-3D-H B + VMT (Figure 7). Therefore, it is important to notice that to be able to deposit the low-emissivity coating by PVD and also fill the cells of the core created by the design with H B + VMT, the top skin and the core and bottom skin have to be printed separately. Only the 3D-air sample can be printed in one step.

4.1.3. Deposition of a Low-Emissivity Coating. Prior to coating deposition, the substrates were cleaned with ethanol in an ultrasonic bath for 5 min, then fixed in the chamber on the sample holder in front of the target using Kapton adhesive, and sputter cleaned in the argon plasma for 20 min. During this step, the pressure was set at 0.3 Pa and the RF power at 200 W. This step is meant to enhance the adhesion of the metal to the polymer. Then, for both IR-3D-air and IR-3D-H B + VMT, the low-emissivity coating composed of a layer of aluminum protected by a thin layer of alumina (Al_2O_3) on top was deposited sequentially on the top skin using a DEPHIS4 (DEPHIS, Etupes, France) pulsed DC magnetron sputtering machine. Aluminum was deposited in metallic mode by sputtering a pure aluminum target with a diameter of 20 cm (A.M.P.E.R.E. industry, Saint-Ouen-l'Aumône, France) in an atmosphere of pure argon. The argon flow rate was set at 100 sccm, and the Al discharge current was 1 A. After 30 min, oxygen was introduced in the chamber with a flow rate of 20 sccm to deposit Al_2O_3 via reactive sputtering for 60 min. No bias is performed during deposition. A whole cycle lasts for
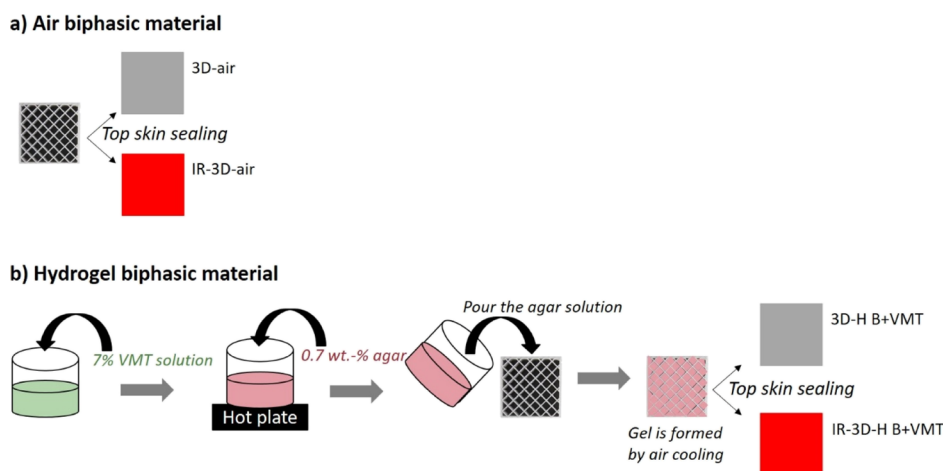
Figure 7. Description of (a) air, (b) hydrogel sandwich multimaterials preparation.

about 3 h. Deposition was also carried out simultaneously on glass for visual control.

4.1.4. 3D-Printed Sandwich Multimaterial Assembly. To prepare the sandwich multimaterial, and especially for 3D-H B + VMT and IR-3D-H B + VMT, H B + VMT has to be prepared. A 7.8 wt % solution in water of dispersed Microlite 963 ++ VMT clay (Specialty Vermiculite Corp., Enoree, South California, United States) was used to prepare H B + VMT. This solution was diluted with distilled water at 7 wt % and heated at 100 °C. When the boiling temperature is reached, 0.7 wt % agar (Mccormick, Baltimore, Maryland, United States) is added and dissolved. This solution composed of agar and VMT is then poured into the cells present in the sandwich polymer core created by the design. Finally, the solution is cooled down at room temperature enabling the formation of hydrogel (Figure 7).

To design the sandwich materials, the top section (with or without low-emissivity coating, depending on the samples studied) is then deposited on the core and sealed by fusing it at 200 °C to the edges of the 3D-printed polymer plate. Therefore, four samples were prepared and their name and composition are shown in Table 3.

4.2. Fire Testing. A mass loss cone calorimeter (Fire Testing Technology, West Sussex, United Kingdom) was used to evaluate the HRR of materials studied upon burning[12] according to the American Society for Testing and Materials (ASTM) E 906. The equipment is similar to that of a cone calorimeter (ASTM E-1354-90), the only difference is the use of a thermopile in the chimney to obtain the HRR rather than employing the oxygen consumption principle. $50 \times 50 \times 3$ mm^3 plates were placed horizontally on a ceramic backing board at a distance of 35 mm from the cone heater. Samples were then exposed to an external heat flux of 50 kW/m², which corresponds to the last stage of a developing fire scenario. All experiments were carried out using a piloted ignition (an electric arc of 32 nA). When the ignition occurs, the electric arc is removed. During the fire test, the HRR is measured as a function of time using a data acquisition system (MLC Calc software, Radcal, Monrovia, California, United States of America). Three main parameters were determined using this test: the TTI, the THR, and the pHRR. THR and pHRR have to be reproducible within ±10% and TTI to ±15%. As a consequence, experiments were performed at least in triplicate

to ensure the repeatability of the results, and the data reported in this work are the average of the three replicated experiments.

Moreover, to obtain additional information, the temperature at the backside of the samples was measured as a function of time during the heat exposure using a K-type thermocouple (TC SA, Dardilly, France) fixed in a calsil plate (to ensure its steadiness during the test) placed under the sample (Figure 8). Data were recorded using a graphtec 34970A data logger (Keysight Technologies, Santa Rosa, CA, USA).
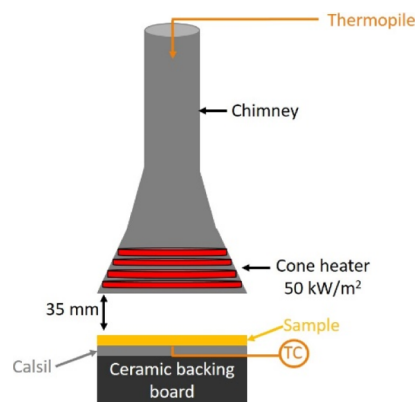

Figure 8. MLCC test.

4.3. Characterization. *4.3.1. Quantitative Values.* The weight, the hydrogel amount, and the thickness (using a ruler placed vertically) of all samples were measured before fire testing to compare the samples with each other.

4.3.2. Emissivity Measurement. Directional hemispherical emissivity of the surfaces was measured by IR diffuse reflectance. The measurements were performed at 20 °C on a Vertex 70v spectrophotometer (Bruker, Bellerica, MA, USA) equipped with a 75 mm-large, gold-coated integrating sphere (Bruker A562). 128 scans from 350 to 7500 cm^{-1} were performed with a resolution of 4 cm^{-1}, and the results were integrated between 7.5 and 13 μm. The beam comes from a SiC light source, goes through a KBr beam splitter at an aperture of 6 mm, and impacts the sample at an angle of 13°. The results were interpreted on the Bruker OPUS software (black body emission calculated at 20 °C), also used to run the spectrophotometer. The emissivity values are presented as the

average of four measurements on different places of the samples to check for repeatability.

4.3.3. Scanning Electron Microscopy Observations. A JEOL JSM 7800F LV scanning electron microscope (JEOL ltd, Tokyo, Japan) was used to confirm the composition of a low-emissivity coating and its thickness. Low-emissivity coating was deposited on a glass slide (using the same setup described in Section 4.3.2), and cut using a blade and a hammer. Using this protocol, a brittle fracture was obtained without affecting the integrity of the sample. The cross-cut samples obtained were then carbon coated with a Bal-Tec SCD005 sputter coater (Bal-Tec, Los Angeles, California, United States). X-ray mappings were performed using an Oxford Instruments SDD EDS detector (Abingdon, United Kingdom), coupled with Aztec software. Al, O, and Si elements were studied. All EDS spectra, EDS maps, and the images obtained were treated using Aztec software afterward.

◼ AUTHOR INFORMATION

Corresponding Author

Serge Bourbigot − *Université Lille, CNRS, INRAE, Centrale Lille, UMR 8207—UMET—Unité Matériaux et Transformations, F-59000 Lille, France;* ⓞ orcid.org/0000-0003-1536-2015; Phone: +33 (0)3 20 43 48 88; Email: serge.bourbigot@univ-lille.fr

Authors

Laura Geoffroy − *Université Lille, CNRS, INRAE, Centrale Lille, UMR 8207—UMET—Unité Matériaux et Transformations, F-59000 Lille, France*

Anne-Lise Davesne − *Université Lille, CNRS, INRAE, Centrale Lille, UMR 8207—UMET—Unité Matériaux et Transformations, F-59000 Lille, France*

Fabrice Parent − *ICD LASMIS, Université de Technologie de Troyes, UMR6281, CNRS, Antenne de Nogent, Pôle Technologique de Haute-Champagne, 52800 Nogent, France; NICCI, LRC CEA-ICD LASMIS, UTT, Antenne de Nogent-52, Pôle Technologique de Haute-Champagne, 52800 Nogent, France*

Frédéric Sanchette − *ICD LASMIS, Université de Technologie de Troyes, UMR6281, CNRS, Antenne de Nogent, Pôle Technologique de Haute-Champagne, 52800 Nogent, France; NICCI, LRC CEA-ICD LASMIS, UTT, Antenne de Nogent-52, Pôle Technologique de Haute-Champagne, 52800 Nogent, France*

Fabienne Samyn − *Université Lille, CNRS, INRAE, Centrale Lille, UMR 8207—UMET—Unité Matériaux et Transformations, F-59000 Lille, France*

Maude Jimenez − *Université Lille, CNRS, INRAE, Centrale Lille, UMR 8207—UMET—Unité Matériaux et Transformations, F-59000 Lille, France;* ⓞ orcid.org/0000-0002-0372-1503

Complete contact information is available at:
https://pubs.acs.org/10.1021/acsomega.0c02902

Author Contributions

L.G wrote this paper and conceived the 3D design, extruded the polymer, printed the samples, and carried out MLCC tests. She also prepared the final samples and carried out and interpreted the fire tests. Fr.S and F.P brought their expertise on PVD and performed the deposition of the low-emissivity coatings by pulsed DC magnetron sputtering. A-L.D. conceived the low-emissivity coating and wrote the Emissivity Measurement section of the paper. Fa.S, M.J, and S.B. supervised the work, discussed the results, and contributed in writing the paper. All authors have given approval to the final version of the manuscript.

Notes

The authors declare no competing financial interest.

◼ REFERENCES

(1) Yang, G.; Wu, W.-H.; Wang, Y.-H.; Jiao, Y.-H.; Lu, L.-Y.; Qu, H.-Q.; Qin, X.-Y.; et al. Synthesis of a novel phosphazene-based flame retardant with active amine groups and its application in reducing the fire hazard of Epoxy Resin. *J. Hazard. Mater.* **2019**, *366*, 78−87.

(2) Ai, L.; Chen, S.; Zeng, J.; Liu, P.; Liu, W.; Pan, Y.; Liu, D.; et al. Synthesis and flame retardant properties of cyclophosphazene derivatives containing boron. *Polym. Degrad. Stab.* **2018**, *155*, 250−261.

(3) Salmeia, K. A.; Gooneie, A.; Simonetti, P.; Nazir, R.; Kaiser, J.-P.; Rippl, A.; Hirsch, C.; Lehner, S.; Rupper, P.; Hufenus, R.; Gaan, S.; et al. Comprehensive study on flame retardant polyesters from phosphorus additives. *Polym. Degrad. Stab.* **2018**, *155*, 22−34.

(4) Wen, Y.; Cheng, Z.; Li, W.; Li, Z.; Liao, D.; Hu, X.; Pan, N.; Wang, D.; Hull, T. R.; et al. A novel oligomer containing DOPO and ferrocene groups: Synthesis, characterization, and its application in fire retardant epoxy resin. *Polym. Degrad. Stab.* **2018**, *156*, 111−124.

(5) Geoffroy, L.; Samyn, F.; Jimenez, M.; Bourbigot, S. Innovative 3D printed design to conceive highly fire-retardant multi-material. *Polym. Degrad. Stab.* **2019**, *169*, 108992.

(6) Geoffroy, L.; Samyn, F.; Jimenez, M.; Bourbigot, S. Additive manufacturing of fire-retardant ethylene-vinyl acetate. *Polym. Adv. Technol.* **2019**, *30*, 1878−1890.

(7) Geoffroy, L.; Davesne, A.-l.; Bellayer, S.; Blanchard, F.; Richard, E.; Samyn, F.; Jimenez, M.; Bourbigot, S.; et al. 3D printed sandwich materials filled with hydrogels for extremely low heat release rate. *Polym. Degrad. Stab.* **2020**, *179*, 109269.

(8) Takahashi, F.; Abbott, A.; Murray, T. M.; T'ien, J. S.; Olson, S. L. Thermal response characteristics of fire blanket materials. *Fire Mater.* **2014**, *38*, 609−638.

(9) Schartel, B.; Beck, U.; Bahr, H.; Hertwig, A.; Knoll, U.; Weise, M. Sub-micrometre coatings as an infrared mirror: A new route to flame retardancy. *Fire Mater.* **2012**, *36*, 671−677.

(10) Försth, M.; Zhao, S.; Roos, A. Spectrally selective and adaptive surfaces for protection against radiative heating: ITO and VO 2. *Fire Mater.* **2014**, *38*, 111−124.

(11) Davesne, A.-L.; Bensabath, T.; Sarazin, J.; Bellayer, S.; Parent, F.; Samyn, F.; Jimenez, M.; Sanchette, F.; Bourbigot, S.; et al. Low-Emissivity Metal/Dielectric Coatings as Radiative Barriers for the Fire Protection of Raw and Formulated Polymers. *ACS Appl. Polym. Mater.* **2020**, *2*, 2880−2889.

(12) Schartel, B.; Hull, T. R. Development of fire-retarded materials-Interpretation of cone calorimeter data. *Fire Mater.* **2007**, *31*, 327−354.